Interactions between hydrated cement pastes and aggressive ammonium: experimental batches characterization

Marie Giroudon, Cédric Roosz, Mehdi Bista, Matthieu Peyre Lavigne, Laurie Lacarrière, Alexandra Bertron

Interactions between hydrated cement pastes and aggressive ammonium: experimental batches characterization

Marie Giroudon[1,*], *Cédric* Roosz[1], *Mehdi* Bista[1], *Matthieu* Peyre Lavigne[2], *Laurie* Lacarrière[1] and *Alexandra* Bertron[1]

[1]LMDC, Université de Toulouse, UPS, INSA Toulouse, France
[2]TBI, Université de Toulouse, CNRS, INRA, INSA, Toulouse, France

Abstract. Agricultural and food industries concrete facilities face chemically aggressive conditions that can damage their microstructure and reduce their lifespan. They are particularly exposed to ammonium-rich environments from natural microbial activity. The poorly crystalline mineralogy of hydrated cement pastes, the compositional variability of the phases and their reactivity make the geochemical behaviour of such materials difficult to investigate and predict over both large periods of time and wide variety of chemical compositions. This work aims (i) to assess the stability of the cement phases involved in ammonium-rich conditions as well as to identify the alteration products, and (ii) to understand the mechanisms and intensity of alteration. To do this, experiments were carried out both on OPC paste powder and on monolithic OPC pastes, degraded by an ammonium nitrate solution in semi-batch conditions. The powder was gradually added to the aggressive solution while the monoliths were immersed for 16 weeks in regularly renewed solution. The pH and the concentration of the chemical elements in solution were monitored over the experiments. The microstructural, chemical and mineralogical changes of the samples were analysed by scanning electron microscopy, electron probe micro-analysis and X-Ray diffraction and showed phenomena of dissolution, leaching and carbonation.

1 Introduction

Ammonium, coming from natural microbial activities, is found in numerous environments such as marine environments [1], livestock waste [2], wastewater [3], agro-food waste as well as in the liquid phase of anaerobic digestion plants that treat this waste [4].
Thus, whether it is to build marine structures or waste treatment storage pits, concrete directly faces ammonium-rich environments. However, the ammonium ion is aggressive to concrete by causing leaching and decalcification of the cementitious matrix [5–7].
Although the deterioration induced by ammonium has been investigated in the literature, most of the experiments was carried out with highly concentrated ammonium nitrate solutions (6 mol/L or more) [8–10] in order to provide accelerated tests of pure water leaching and did not correspond to the parameters encountered in natural environments.
This work aims to understand the mechanisms of deterioration of cementitious pastes immersed in a weakly concentrated ammonium solution and to assess the stability of the cement phases involved in such chemical conditions. For this, the experimental protocol developed combines leaching tests on monoliths and powdered OPC paste, the latter in order to get rid of the diffusion and thus better highlight the chemical reactions of degradation.

* Corresponding author: marie.giroudon@insa-toulouse.fr

2 Material and methods

2.1 OPC paste

2.1.1 Monolithic OPC pastes

CEM I 52.5R (OPC) pastes were made with a water/cement mass ratio of 0.30 and mixed according to the French Standard NF EN 196–1 [11] without adding sand: low speed (140 ± 5 rpm) for 60 s and high speed (285 ± 10 rpm) for 90 s. The specimens were cast in cylindrical plastic moulds 70 mm high and 35 mm in diameter, closed with plastic caps during a 28-day endothermic cure in a tempered room. The water porosity of the OPC paste was measured according to the NF P18-459 standard [12] and was 32.0%.

2.1.2 Powdered OPC paste

After the cure, the same cylindrical specimens as used for the monolithic OPC paste were crushed (using a jaw crusher Restch Type BB51 WC, then a disc crusher Restch Type RS100 and finally an agate mortar) until all the powder passed through an 80 µm sieve. The powder obtained was stored in a desiccator under vacuum until use.

2.2 Aggressive solution

It was chosen to use an ammonium nitrate solution to simulate the attack by the NH_4^+ ion. The concentration of the solution was selected according to the results of previous experiments on anaerobic digestion in laboratory [13–15] in order to faithfully represent a real ammonium concentration found in an agricultural environment. It was chosen not to buffer the solution to avoid additional chemical compounds that could interact with the OPC paste. Thus, the solution used was a 0.0444 mol/L solution of NH_4NO_3 (equivalent to 800 mg/L of NH_4^+).

2.3 Tests methods

2.2.1 Experiments with monolithic pastes

Four cylindrical samples were immersed in 2.5 L of solution, kept at 20 °C in closed plastic containers. pH was measured regularly (daily at the start of the experiment and several times a week thereafter) and the solution was renewed as soon as the pH exceeded 8.6. A few mL of solution was sampled at each renewal for further analyses. Analyses of the degraded pastes were carried out at the end of the experiment.

2.2.2 Experiments with OPC paste powder: Semi-batch

These experiments were carried out in order to enrich the experimental data and to better understand the mechanisms of degradation. The experiments were performed in duplicate and took place in a room at 20°C. The solution was inserted into a hermetically sealed reactor equipped with an inlet to place a pH probe. Air was forced out of the reactor by nitrogen to prevent carbonation during the experiment. OPC powder was added in 100 steps of 1 g (during the duplicate experiment, the additions were made in 1/2 steps from 0 to 10 g for more precision). Thus, at the end of the experiment, a liquid/solid ratio of 20 was reached. The pH was measured every minute and each new addition of powder was made once the pH was stable (chemical equilibrium reached). The experimental device is presented in Figure 1.
Samples of the liquid were taken at certain steps of the experiment: ½; **1**; 2; 3; 4; 5; 6; 7; 8; 9; 10; 11; 12; **13**; 14; 16; 20; 60; 100 (steps in bold letters are those for which the analyses were only made during the duplicate experiment) and were analysed. In order to provide a better knowledge of the solid fraction over time, additional solid phase characterization tests were carried out. OPC paste powder was added to an ammonium nitrate solution with stirring in order to respect the solid/liquid ratio corresponding to steps 7, 12 and 20 of the main experiment. Once the pH stabilized, each samples was centrifuged, solutions and solid was then analysed.

Figure 1. Experimental device for the study of the degradation of OPC paste powder by an ammonium nitrate solution

2.2.3. Analyses

The composition of the liquid samples was analysed by inductively coupled plasma / optical emission spectroscopy ICP-OES spectroscopy (Optima 7000DV ICP/OES Perkin Elmer) (Ca, Al, Si, Mg, Fe) and high performance ion chromatography HPIC (Dionex Thermo Electron ICS 300, CS16 column) (SO_4^{2-}).
For monoliths analyses, the upper part of a sample was carefully sawn off with a diamond saw and then split in two. One half was used for X-Ray Diffraction (XRD) analyses (Brucker D8 Advance, Cu anti-cathode, 40 kV, 40 nA) and the other was used for Scanning Electronic Microscopy (SEM) (JEOL JSM-LV, 15 kV) analyses and Electron Probe Micro-Analysis (EPMA) (Cameca XFive, 15 kV, 20 nA) analyses.
To recover the degraded powder, the solutions were centrifuged (Heraus Megafuge 1.0 Centrifuge), then the powder was dried by solvent exchange by immersion in isopropanol, followed by placing in a desiccator under vacuum. The powders were analysed by XRD.

3 Results

3.1 Experiments with monolithic pastes

3.1.1. pH evolution

The initial pH measured for this solution was 5.65 but it rose very quickly to values between 8.5 and 9.3 when in contact with the monolithic pastes. Each renewal of solution brought the pH back down to its initial value.

3.1.2. Leaching of chemical elements in solution

At the end of the 16 weeks experiment, each cement paste specimen (approximately 120 g of cement paste) had leached mainly calcium, up to 166±18 mmol/L, and also silicon (5.1±0.6 mmol/L), potassium (5.3±0.6 mmol/L), sodium (2.1±0.2 mmol/L) and sulphates (0.5±0.6 mmol/L) but no aluminium nor iron.

3.1.3. Chemical, mineralogical and microstructural changes of the monolithic OPC paste

The chemical composition of the OPC paste is presented in Figure 2, together with a BSE-mode SEM image of the sample. XRD mineralogical analyses were also carried out on these samples even if the diffractograms are not presented here.

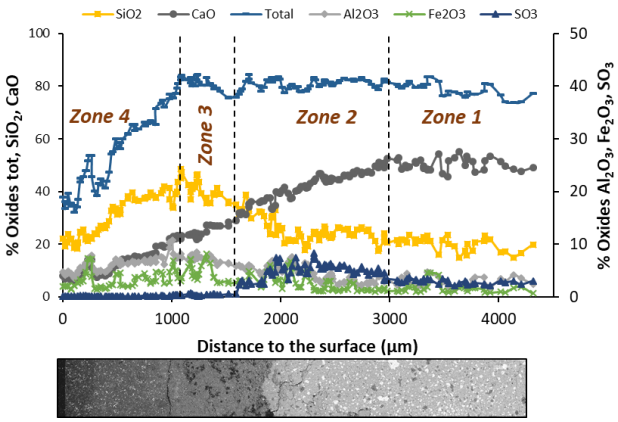

Figure 2. Chemical composition of the OPC paste after 16 weeks of immersion according to the distance to the surface (EPMA), and SEM observations of the polished section in back-scattered electron (BSE) mode.

Four zones are distinguished:
- Zone 1 (from 3000 µm deep) has similar composition to that of a sound specimen with portlandite, ettringite, remaining C_2S, C_3S and C_4AF, mainly made of calcium and shows a high density.
- Zone 2 (from 1590 µm to 3000 µm deep) shows the beginning of the decrease of the calcium content together with a sulphur enrichment. Portlandite is dissolved and the sulphur enrichment is associated with the intensification of the ettringite peaks in the XRD diagram. Small cracks are observed in the SEM image.
- Zone 3 (from 1090 to 1590 µm deep) is a transition zone: the calcium content is still decreasing and there is no longer sulphur in the OPC paste. The total oxides content remains high. At this depth, there is no more portlandite but calcite precipitates and cohabits with some ettringite and the remaining anhydrous phases. Tis zone shows a poor density in the SEM image.
- Zone 4 (until 1090 µm deep) is the external zone. The contents of the main oxides decrease (calcium and silicon), which causes the total oxide content to drop. The main phase of this external zone is calcite, with few brownmillerite and ettringite. The SEM image shows a particularly low density with some brighter zones that could corresponds to the precipitation of calcite crystals.

3.2 Experiments with OPC paste powder

3.2.1. pH evolution

Figure 3 shows the evolution of the pH during the experiment. A first jump in pH associated with the first addition of cement was observed. After that, the pH linearly increases until 10 grams of addition and then keeps increasing less intensely until a plateau is reached at a pH of about 13.

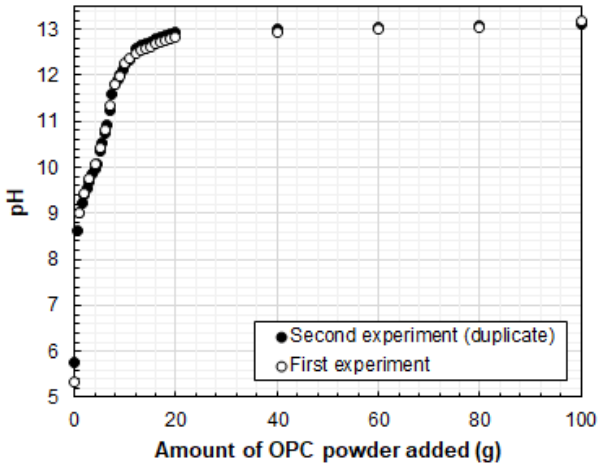

Figure 3. Evolution of the pH of the solution according to the mass of OPC paste powder added

3.2.2. Leaching of chemical elements in solution

Figure 4 presents the experimental results related to the concentrations of calcium (Figure 4.A), silicon and magnesium (Figure 4.B), aluminium and iron (Figure 4.C), and sulphates (Figure 4.D) during the experiment.
The elements have been distributed on four different graphs according to the evolution of their concentration.
The results of the two duplicates are presented together on the graphs, only the measurement of the sulphates content could not be made during the first experiment.
The calcium concentration (Figure 4.A) increases sharply until the 10th gram of addition then increases with a lower slope, until reaching a maximum concentration of 40.7 ± 0.6 mmol/L. Even if the calcium concentrations are significantly higher than the other elements' concentrations, only a small part of the initial total calcium has been leached in the solution (about 81.4 mmol or 3262 mg whereas the 100 g of powder contain about 66.2 g or 1.65 mol of calcium).

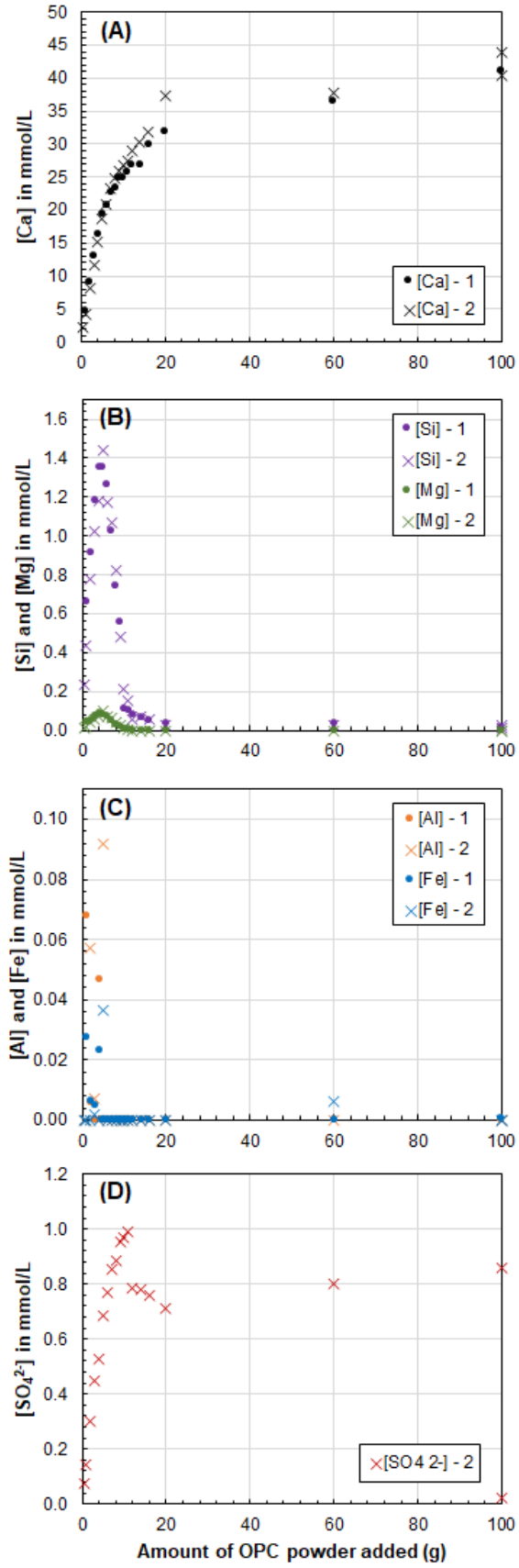

Figure 4. Concentration of calcium (A), silicon and magnesium (B), aluminium and iron (C) and sulphates (D) measured in the solution receiving the OPC paste powder over the experiment

Silicon and magnesium concentrations (Figure 4.B) increase rapidly until addition 5 reaching values of 1.40 ± 0.06 and 0.09 ± 0.07 mmol/L respectively. The concentrations then decrease significantly up to 10 g of addition. This evolution is probably linked to the dissolution of these elements in solution up to the 4th gram of addition, then to the precipitation of phases rich in silicon and magnesium up to the 10th gram. The concentration in silicon then decreases up to the 20th gram and seems to stabilize at a low concentration of about 0.03 mmol/L up to the 10th addition. The final value is close to the detection threshold.

The aluminium and iron concentrations (Figure 4.C) are very low throughout the experiment (below 0.1 mmol/L) and reach their maximum at the very beginning of the addition of powder. After the 5th gram of addition, the concentrations of these elements are below the detection threshold.

The sulphates concentration (Figure 4.D) strongly increases until the 11th gram of addition (from 0 to 1 mmol/L) then it suddenly drops to 0.8 mmol/L and remains between 0.7 and 0.8 mmol/L until the end of the experiment.

3.2.3. OPC powder analyses

The diffractograms (XRD analyses) made on the initial powder as well as on the suspended solids samples taken during the experiment are shown in the Figure 5.

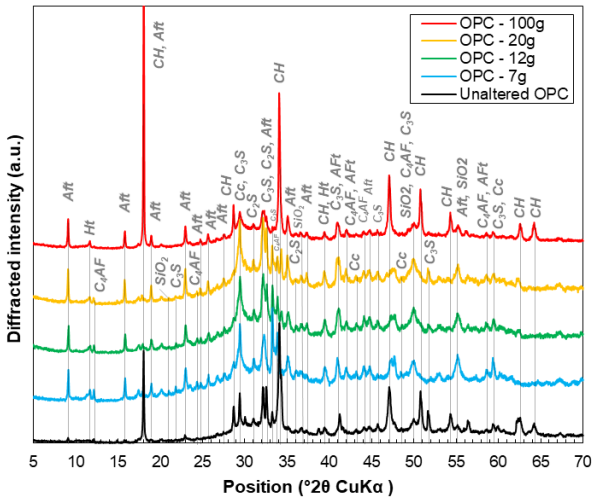

Figure 5. Diffractograms of unaltered OPC powder and solid suspensions during the experiment

The samples were taken after pH stabilization, and correspond to cumulative added masses of 7, 12, 20 and 100 g. The diffractogram of the unaltered OPC powder shows the typical phases of a hydrated OPC, showing in some hydrated phases as portlandite, ettringite, hydrotalcite and C-S-H (large hump visible between 25 and 40 °2Θ) as well as calcite and a small proportion of residual anhydrous (C_2S, C_3S, C_4AF). The degradation of the OPC powder (7 g) results in the dissolution of the hydrates and particularly of the portlandite. In proportion, the peaks attributed to anhydrous peaks appear more intense. The evolution of the degradation (12, 20 and 100

g) shows a progressive decrease of intensity of peaks attributed to the anhydrous phases, coupled with a reappearance of the portlandite.

4 Discussion

4.1 pH evolution

In the monoliths experiment, the pH rose from 5.65 to about 9 at each new renewal. This is coherent with the pH evolution during the OPC powder experiment where the pH rose from about 5.55 to 8.61 then 9.00 respectively, after the first and the second addition of 0.5 g of OPC powder in the two litters of ammonium nitrate solution. These results show that the ammonium nitrate solution, for this concentration, has a very low buffering capacity.
When the pH increases, the equilibrium between NH_4^+ and NH_3 is shifted toward NH_3 (pKa NH_4^+/NH_3 = 9.25). Thus, in the experiment with OPC powder, ammonia becomes the preponderant species in solution from the 2nd gram of addition, even if ammonium remains until a pH of about 12. This change in composition with the pH could therefore partially explain the change in slope on the pH curve (Figure 3) that occurs from a pH of approximately 12: at this pH, only ammonia remains. Thus, at least from pH=12 and perhaps even before, the degradation mechanism of the cement paste cannot be associated with a cation exchange $2\ NH_4^+ \leftrightarrow Ca^{2+}$ as mentioned in the literature [5,6].
The presence of ammonia also explains the very high pH measured at the end of the OPC powder experiment: since ammonia is a strong base, it contributes to the increase in pH in addition to the degradation of the cement.

4.2 Degradation mechanisms (*monoliths*)

The degradation of the monoliths pastes resulted in the progressive decalcification of the paste associated with the dissolution of the Ca-bearing phase portlandite. As a result, calcium was leached into the liquid phase. Surface carbonation was probably due to the presence of dissolved CO_2 (from the air) in solution. A sulphur enrichment was observed in zone 2, probably due to the reprecipitation of ettringite in this zone. The absence of sulphur, the decrease in silicon, and the decrease in calcium in the external zone were coherent with the leaching of chemical elements in solution.

4.3 Contributions of semi-batch experiments

The semi-batch experiments allowed a more precise analysis of the leaching of the elements in solution during the experiment (Figure 4) independently of the effects of diffusion in the material.
Thus, it can be observed that calcium was released throughout the experiment, which is consistent with the progressive and deep decalcification observed on the EPMA profiles of the materials (Figure 2). Magnesium and silicon showed a different behaviour since they were only leached out at the beginning of the experiment (until the 5th gram added) then were consumed. The consumption of magnesium is probably linked to the precipitation of hydrotalcite, detected in the XRD analyses from the 7th gram of addition. These diffractograms also indicate that despite the decalcification of the paste, the C-S-H were not or partially dissolved during the experiment (large hump visible between 25 and 40 °2Θ). This would be consistent with the rise in pH above 12 observed after the first additions, with C-S-H being more stable over these pH ranges [16–18].
Aluminium and iron were leached only on the very first additions and in very small quantities, before being consumed. This is consistent with the monolith experiment where these elements were not detected.
Finally, the sulphates were leached in solution up to the 11th gram added, then a drop in the concentration was observed indicating the precipitation of a sulphate-rich phase. This coincides with the pH of the solution rising above 12. Beyond this value, and considering the concentrations of sulphates in solution, the majority aluminous phase shifts from $Al(OH)_3$ to ettringite [19,20]. The concentrations then remained relatively stable at around 0.8 mmol/L.
It is very likely that aluminium, sulphates (and calcium) indeed precipitated to form ettringite, since an intensification of the peaks associated with ettringite was observed on the diffractograms of the degraded powder (Figure 5), in comparison with the sound paste.
It is possible to draw a parallel between the two experiments: during the first 1 to 5 grams of addition of the experiment with powder, we observe the leaching of the elements in solution (calcium, silicon, sulphates, iron, aluminium, magnesium) which could correspond to the outer zone of the monolith (zone 4). Between 5 and 11 grams of addition, there is a transition zone where silicon and magnesium were not leached anymore whereas sulphates and calcium were still released: it is zone 3. Finally, ettringite precipitated and calcium was still leached: it is zone 2. After the 100th gram of addition, the composition of the OPC powder was close to the one of a sound paste: it is zone 1.

5 Conclusion and perspectives

The attack by the ammonium nitrate solution led to a progressive decalcification of the paste. The semi-batch experiment presented here have shown that the degradation mechanisms observed in the monolithic paste resulted from dissolution and precipitation phenomena. To go further, a more in-depth characterization of the solid as well as an additional thermodynamic modelling work could allow to better understand these phenomena and in particular the associated phases, in order to better understand the complex phenomena of cement paste degradation by ammonium nitrate.

The authors wish to thank the French National Research Agency (ANR) for its financial support in the project BIBENdOM – ANR – 16 – CE22 – 001 DS0602. The authors also thank Maud

Schiettekatte and Vanessa Sonois for their help with the experiment and the analytical support.

References

[1] B.B. Ward, Significance of anaerobic ammonium oxidation in the ocean, Trends Microbiol. **11** (2003) 408–410. https://doi.org/10.1016/S0966-842X(03)00181-1.

[2] N. Zhang, H. Zheng, X. Hu, Q. Zhu, M.S. Stanislaus, S. Li, C. Zhao, Q. Wang, Y. Yang, Enhanced bio-methane production from ammonium-rich waste using eggshell-and lignite-modified zeolite (ELMZ) as a bio-adsorbent during anaerobic digestion, Process Biochem. **81** (2019) 148–155. https://doi.org/10.1016/j.procbio.2019.03.001.

[3] C. Weralupitiya, R. Wanigatunge, S. Joseph, B.C.L. Athapattu, T.-H. Lee, J. Kumar Biswas, M.P. Ginige, S. Shiung Lam, P. Senthil Kumar, M. Vithanage, Anammox bacteria in treating ammonium rich wastewater: Recent perspective and appraisal, Bioresour. Technol. **334** (2021) 125240. https://doi.org/10.1016/j.biortech.2021.125240.

[4] R. Rajagopal, D.I. Massé, G. Singh, A critical review on inhibition of anaerobic digestion process by excess ammonia, Bioresour. Technol. **143** (2013) 632–641. https://doi.org/10.1016/j.biortech.2013.06.030.

[5] G. Escadeillas, H. Hornain, La durabilité des bétons vis-à-vis des environnements chimiquement agressifs, in: *Durabilité Bétons*, Presse de l'ENCP, 2008: pp. 613–705.

[6] G. Escadeillas, Ammonium Nitrate Attack on Cementitious Materials, in: Perform. Cem.-Based Mater. Aggress. Aqueous Environ., Springer, Dordrecht, 2013: pp. 113–130. https://doi.org/10.1007/978-94-007-5413-3_5.

[7] F.M. Lea, The action of ammonium salts on concrete, Mag. Concr. Res. **17** (1965) 115–116. https://doi.org/10.1680/macr.1965.17.52.115.

[8] C. Carde, R. François, J.-M. Torrenti, Leaching of both calcium hydroxide and C-S-H from cement paste: Modeling the mechanical behavior, Cem. Concr. Res. **26** (1996) 1257–1268. https://doi.org/10.1016/0008-8846(96)00095-6.

[9] C. Carde, G. Escadeillas, R. François, Use of ammonium nitrate solution to simulate and accelerate the leaching of cement pastes due to deionized water, Mag. Concr. Res. **49** (1997) 295–301.

[10] C. Perlot, X. Bourbon, M. Carcasses, G. Ballivy, The adaptation of an experimental protocol to the durability of cement engineered barriers for nuclear waste storage, Mag. Concr. Res. **59** (2007) 311–322. https://doi.org/10.1680/macr.2007.59.5.311.

[11] AFNOR, NF EN 196-1. Methods of testing cement - Part 1: Determination of strength, Paris, France, 2016.

[12] AFNOR, NF P18-459. Concrete - Testing hardened concrete - Testing porosity and density, Paris, France, 2010.

[13] M. Giroudon, M. Peyre Lavigne, C. Patapy, A. Bertron, Blast-furnace slag cement and metakaolin based geopolymer as construction materials for liquid anaerobic digestion structures: Interactions and biodeterioration mechanisms, Sci. Total Environ. **750** (2021) 141518. https://doi.org/10.1016/j.scitotenv.2020.141518.

[14] C. Voegel, M. Giroudon, A. Bertron, C. Patapy, M. Peyre Lavigne, T. Verdier, B. Erable, Cementitious materials in biogas systems: Biodeterioration mechanisms and kinetics in CEM I and CAC based materials, Cem. Concr. Res. **124** (2019) 105815. https://doi.org/10.1016/j.cemconres.2019.105815.

[15] M. Giroudon, C. Perez, M. Peyre Lavigne, B. Erable, C. Lors, C. Patapy, A. Bertron, Insights into the local interaction mechanisms between fermenting broken maize and various binder materials for anaerobic digester structures, J. Environ. Manage. **300** (2021) 113735. https://doi.org/10.1016/j.jenvman.2021.113735.

[16] C. Roosz, P. Vieillard, P. Blanc, S. Gaboreau, H. Gailhanou, D. Braithwaite, V. Montouillout, R. Denoyel, P. Henocq, B. Madé, Thermodynamic properties of C-S-H, C-A-S-H and M-S-H phases: Results from direct measurements and predictive modelling, Appl. Geochem. **92** (2018) 140–156. https://doi.org/10.1016/j.apgeochem.2018.03.004.

[17] C.S. Walker, S. Sutou, C. Oda, M. Mihara, A. Honda, Calcium silicate hydrate (C-S-H) gel solubility data and a discrete solid phase model at 25°C based on two binary non-ideal solid solutions, Cem. Concr. Res. **79** (2016) 1–30. https://doi.org/10.1016/j.cemconres.2015.07.006.

[18] J.J. Chen, J.J. Thomas, H.F.W. Taylor, H.M. Jennings, Solubility and structure of calcium silicate hydrate, Cem. Concr. Res. **34** (2004) 1499–1519. https://doi.org/10.1016/j.cemconres.2004.04.034.

[19] C.J. Hampsoim, J.E. Bailey, On the structure of some precipitated calcium alumino-sulphate hydrates, J. Mater. Sci. **17** (1982) 3341–3346. https://doi.org/10.1007/BF01203504.

[20] X. Wang, Z. Pan, X. Shen, W. Liu, Stability and decomposition mechanism of ettringite in presence of ammonium sulfate solution, Constr. Build. Mater. **124** (2016) 786–793. https://doi.org/10.1016/j.conbuildmat.2016.07.135.